buildings

MDPI

Article

The Utilization of Wet Silica Sand Sludge as an Additive in Different Temperature Sustainable Brick Production

Yasemin Tabak

TUBITAK National Metrology Institute (TUBITAK UME), Kocaeli 41470, Türkiye; yasemin.tabak@tubitak.gov.tr; Tel.: +90-262679-4604

Abstract: The conversion of the waste of wet silica sand sludge (W3S) into useful products, such as bricks, glassware, and ceramics, is an alternative solid waste management method. The aim of this study is to determine the effect of silica sand wet sludge additive on brick quality. For this purpose, laboratory-scale brick manufacturing was implemented by using 10%, 30%, 50%, and 100% sludge in clay brick. For proper characterization to understand brick quality, the water absorption, shrinkage, bulk density, compressive strength, and SEM analysis of sintered samples were performed. At the end of the experimental procedure, no negative effects of sludge addition were determined in terms of mechanical strength, porosity, water absorption, or structural integrity. In addition, the incorporation of W3S contributed to sustainable waste management and helped mitigate its environmental impact. Experimental studies revealed that a product with the desired color could be obtained when 50% W3S was used in the mixture. In addition, the optimal composition for making bricks was found to be a mixture of 50% W3S and 50% brick clay, fired at 850 °C. With this mixture, not only is the preferred color achieved, but an optimum balance between mechanical strength, durability, and minimization of environmental damage is also attained. Such a formulation ensures high compressive strength, low porosity, and low water absorption, making it sustainable and a better choice in construction with industrial by-product use. The results obtained are useful in showing possibilities for the solution of environmental problems to utilize waste materials in useful products.

Keywords: brick; building materials; silica sand; sludge; waste

Academic Editor: Andrea Petrella

Received: 3 February 2025
Revised: 4 March 2025
Accepted: 5 March 2025
Published: 8 March 2025

Citation: Tabak, Y. The Utilization of Wet Silica Sand Sludge as an Additive in Different Temperature Sustainable Brick Production. *Buildings* **2025**, *15*, 849. https://doi.org/10.3390/buildings15060849

1. Introduction

Clay has been utilized as a fundamental building material for thousands of years, owing to its unique properties and versatility. The physical and chemical characteristics of clay make it suitable for various construction applications, including bricks, tiles, and plasters [1]. The mineral composition of clay, which often includes kaolinite, quartz, and other minerals, significantly influences its performance as a building material. For instance, the presence of kaolinite contributes to the plasticity and workability of clay, allowing it to be easily molded into desired shapes before firing, which enhances its durability and strength post-processing [2–4]. The composition of clay, particularly the types of clay minerals present, significantly affects the quality of the final product [5].

Brick is a construction material that is known for its relatively high mechanical strength and durability. It is commonly used for building walls and structures. Bricks have been used as a building material throughout history due to their longevity and strength. They can also be recycled and reused in the production of other construction materials. Bricks can be made from various materials, including clay and waste materials such as waste marble

powder and groundnut shell ash [2,3,6,7]. The manufacturing process of bricks typically involves firing processes at high temperatures [4,8]. The firing temperature is another critical factor that influences the characteristics of fired clay bricks. Research indicates that varying the firing temperature can lead to significant changes in the microstructure and physical properties of bricks, such as porosity and compressive strength [9,10]. Conversely, insufficient firing temperatures may result in poor bonding and structural weaknesses, leading to bricks that are prone to cracking and other forms of degradation [11].

Numerous studies have explored the use of waste materials in brick production to promote sustainability and address waste management challenges. Various materials, including cotton waste, textile sludge, rice husk ash, fly ash, paper residues, and agricultural and plastic waste, have been incorporated into bricks to enhance their properties and reduce landfill waste [12–17]. Researchers have also investigated the use of plastic waste, mycelium-based composites, and natural phosphate waste in brick manufacturing, highlighting their potential for creating eco-friendly construction materials. Studies like those by Weng et al., Chen and Wu have demonstrated that incorporating sludge and other industrial by-products can maintain or improve brick properties, such as compressive strength, density, and shrinkage, while meeting regional standards [18,19]. Similarly, efforts by Uslu et al. and Adiyanto et al. confirm the viability of using chemical treatment sludge and plastic waste in brick production without compromising quality [20,21]. These findings collectively emphasize the potential of utilizing waste materials to develop sustainable, high-quality bricks. Furthermore, innovative approaches, such as the blending of clay with waste materials or other natural additives, are being explored to enhance the performance of clay-based construction products [22,23].

Silica waste sludge, particularly from geothermal sources, offers significant opportunities for recycling and utilization in construction and environmental applications. Geothermal power plants, such as the Dieng Geothermal Power Plant (PLTPB) in Indonesia, generate approximately 160 to 165 tons of silica-rich sludge per month [24,25]. This sludge, primarily composed of amorphous silicon dioxide (SiO_2) with up to 98% purity [26], has been explored for its potential to enhance construction materials, particularly in geopolymer production, as a replacement for traditional components, thereby improving mechanical properties and promoting sustainability [26,27].

Silica waste, primarily originating from industrial processes and agricultural residues, has been extensively studied for its applications in various industries. Kuok et al. investigated the use of recycled waste silica sludge in developing humidity-buffering coatings via a room-temperature sol–gel method, demonstrating energy-efficient recycling with enhanced humidity control and antimicrobial properties [28]. Judith's research highlighted the transformation of industrial waste-derived nanomaterials for environmental cleanup, utilizing silica-rich sludge for removing organic and inorganic contaminants [29]. Additionally, Salman et al. explored the extraction of nano-silica from agricultural waste, providing insights into value-added product development from silica sludge waste [30]. These studies underscore the potential of repurposing natural silica sludge waste into functional materials, contributing to waste reduction and environmental sustainability. The incorporation of waste materials in brick production presents a sustainable solution to waste management challenges while reducing the environmental impact of traditional clay extraction. The interaction between clay composition, firing temperature, and additives is crucial in optimizing brick manufacturing to meet performance standards while mitigating environmental impact.

Ongoing research continues to highlight the importance of silica sludge waste in eco-friendly building practices, reinforcing its role in modern sustainable construction. Therefore, this study aims to determine the maximum utilization ratio of silica sand sludge

to emphasize the importance of waste incorporation in sustainable material development. The raw sand produced in Istanbul's Şile district mining locations by Kumsan Foundry Materials Industry and Trade Inc. is washed, screened, and graded in the green sand enrichment plants in Şile-Sahilköy for easy transportation. The silica sand so processed has a minimum of 98% silica and can be utilized in various industries, including construction, electrical material manufacturing, casting, pipe production, building chemicals, glass manufacturing, sandblasting, and powder metallurgy. In light of increasing environmental awareness, the obligation to manage waste disposal, the lack of storage space, and the high economic costs associated with creating new landfills, there is a growing need for scientific research on reusing similar types of waste. This research looks at the use of silica waste sludge, specifically from geothermal activities, as an alternative method of waste management and recovery of resources. This study focuses on converting waste into valuable materials for applications such as brick manufacturing, while also discussing the properties of different compositions. Other applications could include catalysis, construction, and industrial uses. Therefore, this approach can be promoted as a circular economy that minimizes environmental impact while maximizing resource efficiency.

The aim of this study is clearly articulated. This research investigates the potential utilization of silica waste sludge, particularly from geothermal sources, in the production of sustainable construction materials. By incorporating W3S into brick manufacturing, this study evaluates the impact of varying waste content on the mechanical, physical, and microstructural properties of the final products. The objective is to explore an environmentally friendly approach to waste management and resource recovery, aligning with circular economy principles. The findings of this study aim to contribute to the advancement of green building materials while addressing waste disposal challenges and sustainability concerns in the construction industry.

2. Materials and Methods

The utilization of waste silica sand sludge (W3S) from the green sand plant in Şile, Istanbul, for brick production was investigated. The experimental study involved blending dried brick clay with milled silica sand sludge in varying weight ratios. The mixing process was conducted in a ball mill for 2 h to ensure homogeneity. The prepared mixture was then incrementally blended in a mixer bowl, with water sprayed gradually until a dough-like consistency was achieved. The resulting dough was stored in plastic bags for 2 days in a sealed environment at approximately 20 °C for curing. After curing, the dough was placed in a vacuum extrusion chamber and pressed into shape. The formed samples were dried under humidity-free conditions by placing them in a drying cabinet at room temperature for 3 to 4 days. The pressing process was carried out using a laboratory-scale uniaxial dry press machine, with samples mixed with 5% water to enhance workability. Subsequently, 10%, 30%, 50%, and 100% W3S mixtures were blended with brick clay and compressed at a pressure of 25 bar. The desiccated samples were then oven-dried for 24 h, with the temperature gradually increasing from ambient to 100 °C.

The sintering process was conducted in a intering furnace (Protherm, İstanbul, Türkiye) at three different temperatures: 800 °C, 850 °C, and 900 °C. The heating regime involved a controlled temperature increase of 2 °C per minute, followed by a 3 h hold at the target temperature before being cooled at the natural cooling rate of the furnace.

The physical and mechanical properties of the manufactured bricks were analyzed to determine the optimal mixing ratio and firing temperature. Key parameters, such as dry shrinkage, firing shrinkage, dry weight loss, sintered weight loss, and dry strength, were assessed by measuring the dimensions and weights of the samples at different stages of

processing (raw, drying, and firing). Additionally, the sintered samples were evaluated for water absorption, density, porosity, and firing strength.

In the experimental studies, brick clay was obtained from İkizler Brick Industry (Kocaeli, Türkiye), which operates in İzmit/Kocaeli, while wet silica sand sludge (W3S) was supplied by Kumsan Foundry Materials Industry and Trade Inc. (İstanbul, Türkiye) Prior to use, the W3S material was dried in an oven. After drying, each sample was thoroughly mixed and then prepared for experiments by applying the pouring–quadrupling method to reduce the sample size before allowing it to rest. To characterize the raw materials used in this study, various analyses were conducted. The physical properties of sand and W3S are presented in Table 1, while their semi-quantitative elemental compositions and wet chemical analysis results are provided in Tables 2 and 3, respectively. Additionally, mineralogical analysis was performed on the brick clay + W3S mixture, with the results summarized in Table 4. The wet chemical analysis results for this mixture are detailed in Table 5.

Table 1. Physical properties of sand and W3S.

Property	Result of Sand	Result of W3S
Moisture, %	2.69	44
Theoretical Density, g/cm^3	2.6425	2.7582
Bulk Density, g/cm^3	1.470	0.20

Table 2. Semi-quantitative elemental analysis of sand and W3S.

Element	Amount (%) of Sand	Amount (%) of W3S
Si	43.541	30.072
Al	0.312	15.438
Fe	0.093	3.092
Ti	0.030	0.384
Ca	0.051	0.086
Mg	0.427	0.258
K	0.042	0.450
O	55.330	49.993
N	-	0.031
Total	99.826	99.804

Table 3. Wet chemical analysis of silica sand and W3S.

Compound	Amount (%)	Amount (%) of W3S
SiO_2	97.927	59.452
Al_2O_3	0.604	26.956
Fe_2O_3	0.145	4.086
TiO_2	0.054	0.593
CaO	0.078	0.110
MgO	0.734	0.396
K_2O	0.056	0.501
Na_2O	-	0.039
Loss on Ignition	0.200	7.590
Total	99.798	99.723

In Table 1, the moisture content of sand is relatively low (2.69%), whereas W3S exhibits a significantly higher moisture content of 44%. This suggests that W3S has a higher water retention capacity, which may influence its workability and behavior in various applications. The theoretical density values are quite similar, with sand having a density of 2.6425 g/cm^3

and W3S at 2.7582 g/cm^3. However, the bulk density of sand (1.470 g/cm^3) is much higher than that of W3S (0.920 g/cm^3), indicating that W3S has a more porous structure, possibly due to its finer particle size or a more complex internal microstructure.

Table 4. Mineralogical analysis results of brick clay + W3S mixtures.

W3S%10 + Brick Clay% 90	W3S% 30 + Brick Clay% 70	W3S% 50+ Brick Clay% 50	W3S%100	Brick Clay
Quartz, SiO_2 Calcite, $CaCO_3$ Feldspar İllite $(K,H_3O)Al_2Si_3AlO_{10}(OH)_2$ Montmorillonite $CaO_2(Al,Mg)_2Si_4O_{10}(OH)_2\cdot 4H_2O$ Cristobalite, SiO_2 Almandine, $Fe_3Al_2(SiO_4)_3$	Quartz, SiO_2 Calcite, $CaCO_3$ Feldspar İllite $(K,H_3O)Al_2Si_3AlO_{10}(OH)_2$ Montmorillonite $CaO_2(Al,Mg)_2Si_4O_{10}(OH)_2\cdot 4H_2O$ Cristobalite, SiO_2 Almandine, $Fe_3Al_2(SiO_4)_3$	Quartz, SiO_2 Calcite, $CaCO_3$ Feldspar İllite $(K,H_3O)Al_2Si_3AlO_{10}(OH)_2$ Montmorillonite $CaO_2(Al,Mg)_2Si_4O_{10}(OH)_2\cdot 4H_2O$ Cristobalite, SiO_2 Almandine, $Fe_3Al_2(SiO_4)_3$	Kaolinite ($Al_2Si_2O_5(OH)_4$ Quartz (SiO_2) Hematite (Fe_2O_3)	Quartz (SiO_2) Calcite ($CaCO_3$) İllite $(K_1H_3O)Al_2Si_3AlO_{10}(OH)_2$ Clinochlorine $(Mg,Fe)_6(Si,Al)_4O_{10}(OH)_8$ Feldspar Gypsum ($CaSO_4\cdot 2H_2O$)

Table 5. Wet chemical analysis results of brick clay + W3S mixtures.

	W3S%10 + Brick Clay% 90	W3S%30 + Brick Clay% 70	W3S%50+ Brick Clay% 50	W3S%100
Compound	**Quantity (%)**	**Quantity (%)**	**Quantity (%)**	**Quantity (%)**
SiO_2	42.905	46.497	49.985	59.452
Al_2O_3	16.462	17.789	19.351	26.956
Fe_2O_3	7.252	6.706	5.922	4.086
TiO_2	0.785	0.748	0.685	0.593
CaO	11.915	9.797	7.462	0.110
MgO	3.960	3.244	2.666	0.396
Na_2O	0.801	0.710	0.526	0.039
K_2O	1.937	1.661	1.421	0.501
SO_3	0.702	0.706	0.597	0.000
P_2O_5	0.161	0.147	0.134	0.107
MnO_2	0.116	0.080	0.063	0.015
Cr_2O_3	0.025	0.036	0.030	0.035
Loss of ignition	12.740	11.680	10.990	7.590
Total	99.763	99.803	99.833	99.880

As shown in Table 2, the elemental composition highlights a stark contrast between the two materials. Sand is predominantly composed of silicon (Si) (43.541%) and oxygen (O) (55.33%), making it highly silica-rich, as expected for quartz-based sands. On the other hand, W3S contains significantly lower silicon (30.072%) and oxygen (49.993%) but has notably higher aluminum (Al) (15.438%), iron (Fe) (3.092%), and titanium (Ti) (0.384%) contents compared to sand. These differences suggest that W3S contains more clay minerals or other aluminosilicate phases, contributing to its lower bulk density and higher moisture retention.

As shown in Table 3, the wet chemical analysis further confirms the dominance of silica in sand, with the SiO_2 content reaching 97.927%. In contrast, W3S has a significantly lower SiO_2 content (59.452%), indicating a more complex mineralogical composition. The Al_2O_3 content in W3S (26.956%) is markedly higher than in sand (0.604%), reinforcing the presence of aluminosilicate phases. Additionally, the Fe_2O_3, TiO_2, and K_2O contents in W3S are significantly higher than those in sand, further differentiating their chemical compositions. Another key difference is the loss on ignition (LOI) value, which is much higher in W3S (7.590%) compared to sand (0.200%). This high LOI value in W3S suggests

the presence of volatile components, such as bound water, organic matter, or carbonates, which decompose upon heating. The comparative analysis of sand and W3S demonstrates that sand is a highly silica-rich material with a dense and less porous structure, while W3S exhibits characteristics of a more alumina-rich material with higher moisture retention, lower bulk density, and a more complex chemical composition. These differences suggest that sand is likely more suitable for applications requiring high-purity silica, such as glass manufacturing or foundry use, while W3S may be better suited for applications where clay or aluminosilicate properties are advantageous, such as ceramics, refractories, or binding agents in construction materials.

The particle size distribution of the material indicates a well-graded composition with a range of particle sizes. With 100% of the particles measuring below 850 microns, the material is relatively fine. The fact that 90% of the particles are smaller than 612.945 microns and 50% are below 360.707 microns suggests a balanced distribution between coarse and fine particles. Additionally, with 10% of the particles being smaller than 210.620 microns, the presence of finer particles is evident, which may influence the material's flowability, packing density, and overall behavior in different applications. The given particle size distribution data indicates that the sludge has a very fine-grained structure. All particles are below 230 microns, with 90% of them being smaller than 74.746 microns, suggesting that the material is predominantly composed of fine particles. The median (D50) value is 10.857 microns, meaning half of the particles are smaller and half are larger than this size. Additionally, with 10% of the finest fraction measuring below 1.165 microns, a significant portion of the material is in the micron range. This distribution suggests that the sludge has a high level of fineness, likely exhibiting plastic properties, high water retention capacity, and potential suspension behavior. The particle size distribution of the two materials reveals distinct differences in their granulometric composition. The first material, with 100% of its particles below 850 microns and a median (D50) value of 360.707 microns, exhibits a well-graded structure with both coarse and fine fractions, ensuring a balanced distribution that may influence flowability and packing density. In contrast, the sludge sample has an extremely fine-grained nature, with all particles below 230 microns and a much lower D50 value of 10.857 microns, indicating a predominance of very fine particles. Additionally, while only 10% of the first material's particles are smaller than 210.620 microns, the sludge contains 10% of its particles below 1.165 microns, highlighting its significantly finer texture. This suggests that the first material may behave more like a granular solid, whereas the sludge, with its high water retention and potential suspension properties, is likely to exhibit plasticity and a more cohesive nature.

Table 4 identifies the mineral content of wet silica sand sludge (W3S) and brick clay in different proportions, hence giving insight into the structural and chemical nature of these materials with respect to the production of bricks. This analysis was conducted using the Shimadzu XRD-6000 (Kyoto, Japan).

The analysis emphasizes the most frequent presence of quartz (SiO_2), calcite ($CaCO_3$), feldspar, illite, montmorillonite, and cristobalite within the mixtures. The results indicate that brick clay is mainly made up of quartz, calcite, feldspar, illite, and clinoclore, while W3S comprises a high content of kaolinite, quartz, and hematite. Incorporating W3S into the brick clay allows the resultant mixtures to retain the mineralogical features of both constituents; however, a novel almandine phase ($Fe_3Al_2(SiO_4)_3$) is identified, particularly at high contents of W3S. The mineralogical change observed shows that the addition of W3S assists in the development of new phases, which can influence the physical and mechanical characteristics of the final brick product. The presence of montmorillonite, a swelling and shrinkage clay mineral, can also influence the plasticity and thermal characteristics of the compositions upon firing. Overall, the mineralogical composition demonstrates the

potential of W3S as a valuable additive in the production of bricks, resulting in the formation of stable and beneficial mineral phases with the potential to enhance the material's properties. However, the presence of hematite in W3S could have some impact on the color development of the end product, as it has been noted that iron oxides can affect fired brick redness.

Table 5 illustrates a chemical analysis of different brick clay–W3S combinations with a description of the composition of the major oxides and how they may impact the material's performance. It is possible to identify a trend as the content of W3S increases with significant variations in the SiO_2, Al_2O_3, Fe_2O_3, and CaO contents. Silicon dioxide (SiO_2) rises progressively from 42.905% in 10% W3S to 59.452% in 100% W3S, reflecting an improvement in the thermal stability and hardness of the material. An increased SiO_2 content can lead to stronger sintering bonds and enhance the mechanical properties of the bricks. The aluminum oxide (Al_2O_3) content rises from 16.462% to 26.956%, which means the refractory and thermal deformation resistance properties are enhanced, making the mixture more suitable for high-temperature use. The iron oxide (Fe_2O_3) content, on the other hand, falls from 7.252% in 10% W3S to 4.086% in 100% W3S, which influences both the color and mechanical strength of the bricks. A decrease in the Fe_2O_3 content will make the bricks lighter in color and can influence bonding strength at sintering. The calcium oxide (CaO) content decreases significantly from 11.915% in 10% W3S to as low as 0.110% in 100% W3S, reducing the fluxing effect during firing. This results in high porosity at higher ratios of W3S, influencing the density and water absorption characteristics of the product. The magnesium oxide (MgO), potassium oxide (K_2O), and sodium oxide (Na_2O) contents also fall with rising W3S, potentially influencing the sintering process and material workability as a whole. The loss on ignition (LOI) percentages drop with rising W3S composition, from 12.740% in 10% W3S to 7.590% in 100% W3S, reflecting less organic and volatile content. This suggests that a higher level of W3S content will lead to a denser and more stable final product if other physical properties, such as porosity and shrinkage, remain within acceptable bounds.

3. Results

The effects of various W3S-to-brick soil ratios and sintering temperatures on the physical and mechanical properties of the samples are highlighted in Tables 6–9. In all the mixtures tested, a rise in sintering temperature generally increases compressive strength while simultaneously reducing porosity and water absorption; however, above some temperature limits, there are minimal gains or minor losses in strength.

Table 6. Aggregated results of the mechanical and physical properties of the samples produced from a mixture of 10% W3S + 90% brick soil.

25 BAR 1/05	**800 °C**	**850 °C**	**900 °C**
Total shrinkage, %	0.46	1.17	0.63
Total weight loss, %	12.60	13.62	13.70
Compression strength, N/mm^2	114.061	115.940	138.992
Water absorption ratio, %	11.26	11.12	11.34
Porosity, %	22.62	22.13	22.38
Density	2.01	1.99	1.97

Table 6 presents the mechanical and physical properties of the samples composed of 10% W3S and 90% brick soil, sintered at 800 °C, 850 °C, and 900 °C. Total shrinkage follows a fluctuating trend, starting at 0.46% at 800 °C, increasing significantly to 1.17% at 850 °C, and then decreasing to 0.63% at 900 °C. Total weight loss increases with tempera-

ture, ranging from 12.60% at 800 °C to 13.70% at 900 °C, indicating progressive material loss. Compressive strength exhibits a notable rise at 900 °C (138.992 N/mm^2), outperforming both 800 °C (114.061 N/mm^2) and 850 °C (115.940 N/mm^2), suggesting that higher temperatures enhance structural integrity. However, water absorption remains relatively stable, fluctuating between 11.12% and 11.34%, indicating minor variations in material compactness. Porosity follows a similar pattern, showing minimal changes between 22.13% and 22.62%, while density slightly decreases from 2.01 g/cm^3 at 800 °C to 1.97 g/cm^3 at 900 °C. These results suggest that 900 °C provides the highest compressive strength, but the slight decrease in density may affect material compactness.

Table 7. Aggregate results of the mechanical and physical properties of the samples produced from a mixture of 30% W3S + 70% brick soil.

25 BAR 1/05	**800 °C**	**850 °C**	**900 °C**
Total shrinkage, %	0.54	1.01	0.72
Total weight loss, %	11.77	12.36	12.43
Compression strength, N/mm^2	113.756	121.949	109.083
Water absorption ratio, %	11.37	11.07	11.09
Porosity, %	22.82	22.14	21.98
Density	2.01	2.00	1.98

Table 8. Aggregate results of the mechanical and physical properties of the samples produced from a mixture of 50% W3S + 50% brick soil.

25 BAR 1/05	**800 °C**	**850 °C**	**900 °C**
Total shrinkage, %	1.60	1.12	1.09
Total weight loss, %	10.88	11.29	11.34
Compression strength, N/mm^2	115.203	126.924	122.038
Water absorption ratio, %	12.10	11.51	11.04
Porosity, %	24.14	22.94	22.26
Density	2.00	1.99	2.02

Table 9. Aggregate results of the mechanical and physical properties of the brick samples produced from 100% W3S.

25 BAR 1/05	**800 °C**	**850 °C**	**900 °C**
Total shrinkage, %	1.12	1.12	1.32
Total weight loss, %	8.15	8.56	8.69
Compression strength, N/mm^2	125.579	105.969	134.400
Water absorption ratio, %	13.43	14.69	13.23
Porosity, %	26.26	28.06	26.21
Density	1.95	1.91	1.98

Table 7 presents the mechanical and physical properties of the samples composed of a 30% W3S and 70% brick soil mixture, sintered at 800 °C, 850 °C, and 900 °C. The results indicate that total shrinkage increases with temperature, reaching its highest value at 850 °C (1.01%) before slightly decreasing at 900 °C (0.72%). Similarly, total weight loss follows an increasing trend, ranging from 11.77% at 800 °C to 12.43% at 900 °C, suggesting higher material loss at elevated temperatures. Compressive strength is observed to be the highest at 850 °C (121.949 N/mm^2), outperforming both 800 °C (113.756 N/mm^2) and 900 °C (109.083 N/mm^2), indicating that 850 °C is the most effective sintering temperature

for strength enhancement. Meanwhile, water absorption remains relatively stable across all temperatures, fluctuating between 11.07% and 11.37%. A slight reduction in porosity is noted with increasing temperature, decreasing from 22.82% at 800 °C to 21.98% at 900 °C, signifying improved densification of the material. However, density exhibits a minor decline, dropping from 2.01 g/cm^3 at 800 °C to 1.98 g/cm^3 at 900 °C, which may indicate microstructural changes affecting the compactness of the samples. Overall, these findings suggest that 850 °C provides the most favorable balance of mechanical and physical properties, optimizing compressive strength while maintaining controlled porosity and shrinkage. Further increases in temperature do not yield significant mechanical benefits and may slightly compromise density and material integrity.

Table 8 presents the mechanical and physical properties of the samples composed of a 50% W3S and 50% brick soil mixture, sintered at 800 °C, 850 °C, and 900 °C. The results indicate that total shrinkage is highest at 800 °C (1.60%) but decreases at 850 °C (1.12%) and slightly further at 900 °C (1.09%), suggesting that higher temperatures contribute to dimensional stability. Similarly, total weight loss exhibits a slight increase with rising temperature, ranging from 10.88% at 800 °C to 11.34% at 900 °C, indicating a gradual material loss. Compressive strength reaches its peak at 850 °C (126.924 N/mm^2), surpassing both 800 °C (115.203 N/mm^2) and 900 °C (122.038 N/mm^2), highlighting that 850 °C provides the most effective sintering conditions for strength enhancement. Water absorption follows a decreasing trend, with values of 12.10% at 800 °C, 11.51% at 850 °C, and 11.04% at 900 °C, indicating improved densification at higher temperatures. A similar pattern is observed in porosity, which declines from 24.14% at 800 °C to 22.26% at 900 °C, further supporting the densification process. Density remains relatively stable, fluctuating between 2.00 g/cm^3 and 2.02 g/cm^3, suggesting that structural integrity is maintained across different sintering temperatures. Overall, these findings indicate that 850 °C is the optimal sintering temperature for a 50% W3S and 50% brick soil mixture, achieving the highest compressive strength while effectively controlling shrinkage, porosity, and water absorption. Further increases in temperature offer minor improvements in water absorption and porosity but do not significantly enhance mechanical strength.

Table 9 outlines the mechanical and physical properties of the samples composed entirely of 100% W3S, sintered at 800 °C, 850 °C, and 900 °C. Total shrinkage remains constant at 1.12% for 800 °C and 850 °C, increasing slightly to 1.32% at 900 °C, indicating moderate thermal expansion. Total weight loss increases marginally with temperature, from 8.15% at 800 °C to 8.69% at 900 °C, suggesting relatively lower material degradation compared to the other mixtures. Compressive strength shows a fluctuating trend, peaking at 125.579 N/mm^2 at 800 °C, dropping significantly at 850 °C (105.969 N/mm^2), and then recovering to 134.400 N/mm^2 at 900 °C, highlighting the importance of sintering conditions. Unlike the other mixtures, water absorption exhibits greater variability, increasing from 13.43% at 800 °C to 14.69% at 850 °C before decreasing again to 13.23% at 900 °C, which may be attributed to changes in microstructure. Similarly, porosity follows an increasing pattern at 850 °C (28.06%) before reducing to 26.21% at 900 °C, suggesting the potential for enhanced densification at higher temperatures. Density remains relatively stable, fluctuating between 1.91 g/cm^3 and 1.98 g/cm^3, indicating that compactness is not significantly altered. These findings suggest that while 900 °C maximizes compressive strength, increased porosity and water absorption at intermediate temperatures may pose challenges for structural applications.

As seen in Table 6, the 10% W3S mixture possesses the maximum compressive strength at 900 °C (138.992 N/mm^2), yet the 50% W3S mixture exhibits the best overall properties at 850 °C, including high strength (126.924 N/mm^2), low porosity, and homogeneous density. On the other hand, the 100% W3S samples possess higher porosity and water absorption

with more inconsistent strength, which shows their lesser application suitability where densification is required. The outcomes indicate that the composition of W3S and the sintering temperature must be optimized to achieve the desired material properties, where the most successful composition is 50% W3S at 850 °C.

The overall shrinkage of the samples exhibits a progressive increase with rising temperature and sludge content. The data in Figure 1 indicate that the 50% W3S + 50% brick soil sample exhibits greater shrinkage at 800 °C than at 850 °C and 900 °C. Notably, in the 100% sludge samples, the shrinkage rate stabilizes at 900 °C, suggesting the presence of a threshold effect, beyond which further temperature increases do not significantly impact dimensional reduction. These findings underscore the critical role of both temperature and sludge content in influencing the dimensional stability of the material.

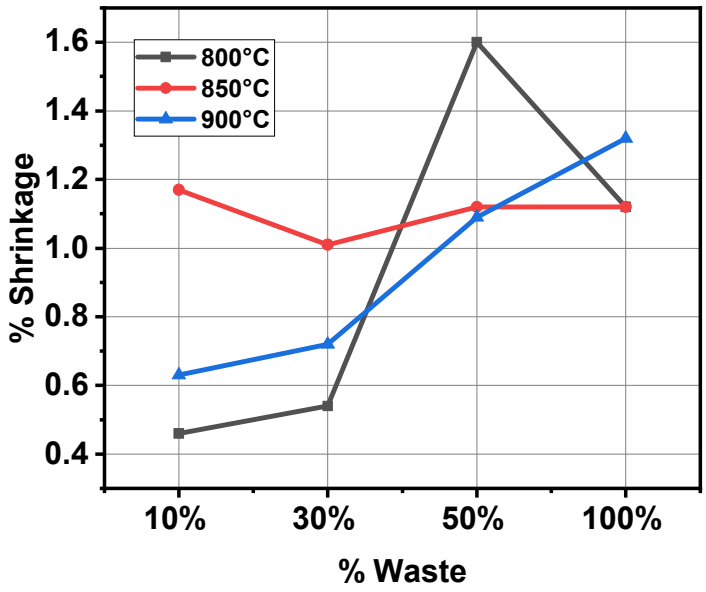

Figure 1. Graph of shrinkage and waste percentage variation at different temperatures.

Figure 2 illustrates the variation in the compressive strength of the samples as a function of waste percentage at different sintering temperatures. In general, at 800 °C, the compressive strength remains relatively stable up to the addition of 50% W3S, while at 850 °C and 900 °C, significant fluctuations are observed depending on the waste content. At 850 °C, the compressive strength initially increases but experiences a sharp decline beyond 50% waste content. The sample containing 50% sludge is observed to exhibit maximum strength at 850 °C. At 900 °C, the highest strength is achieved at 10% waste content, whereas at 30% waste content, the strength decreases before increasing again.

This behavior can be attributed to phase transformations of waste components at elevated temperatures, weakening of the bonding structure, and microstructural changes occurring during the sintering process. In particular, the reduced compressive strength in the samples with high waste content at 900 °C can be associated with the insufficiency of binding phases and increased porosity. These findings highlight the critical impact of waste content and sintering temperature on compressive strength, emphasizing the importance of determining optimal processing parameters [31–33].

As seen in Figure 3, generally, absorption increases linearly with the sludge content but shows relatively small variations with temperature. The lowest absorbing samples are the 10% and 30% ones, which have the best porosity control as well as material compactness. The samples containing 50% and 100% sludge absorb more water, which means that porosity has increased, and the compositions might lose some durability. This behav-

ior indicates that a higher content of sludge tends to create more open microstructures, negatively affecting the material's long-term moisture resistance [34–36].

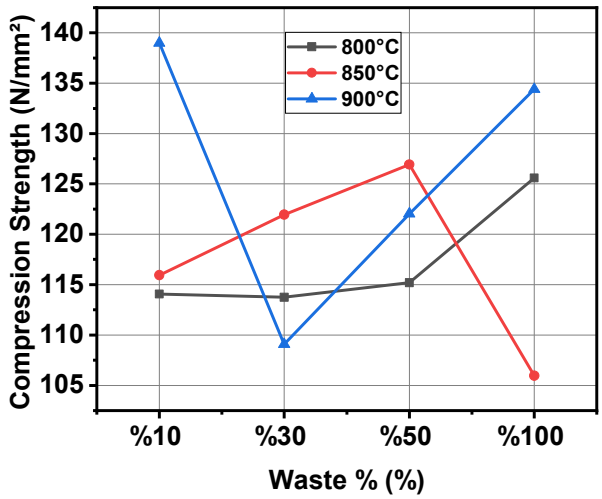

Figure 2. Graph of compression strength and waste percentage variation at different temperatures.

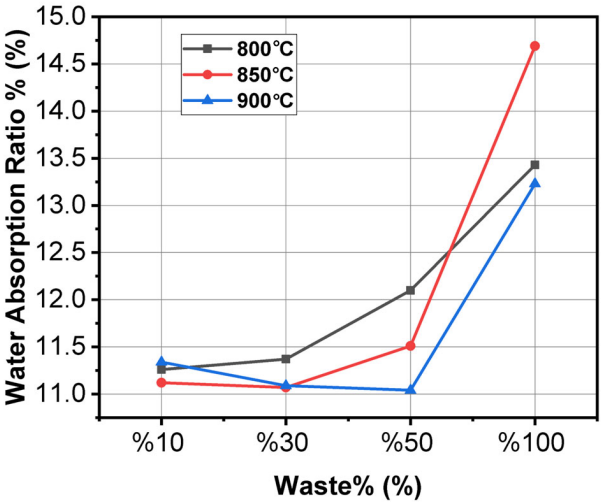

Figure 3. Graph of water absorption and waste percentage variation at different temperatures.

As shown in Figure 4, the porosity of the samples is directly influenced by both the sludge content and the firing temperature. In the case of 800 °C and 850 °C, porosity increases with the increase in sludge ratios, indicating that more voids form in the structure. At 900 °C, however, a slight decrease in porosity was observed for the 50% sludge samples, showing densification effects at higher temperatures. For the 100% sludge samples, porosity remains high even at 900 °C, reflecting the difficulty of achieving a compact structure with excessive sludge content. This underlines the need for an optimum ratio of sludge to balance porosity and material performance [37–39].

As seen in Figure 5, with an increased sludge content, the density values decrease, indicating that the added sludge is lighter than clay. The influence of the firing temperature on density is not very pronounced. Initially, density increases with the rising waste content at all sintering temperatures, reaching its maximum at 50% waste content at 900 °C. However, beyond a certain waste percentage, density starts to decline, particularly at 850 °C and 900 °C, with this decrease being more pronounced at 850 °C. This reduction is likely attributed to phase transformations, thermal degradation, or insufficient bonding between the waste particles and the clay matrix, leading to excessive porosity formation [33,40,41].

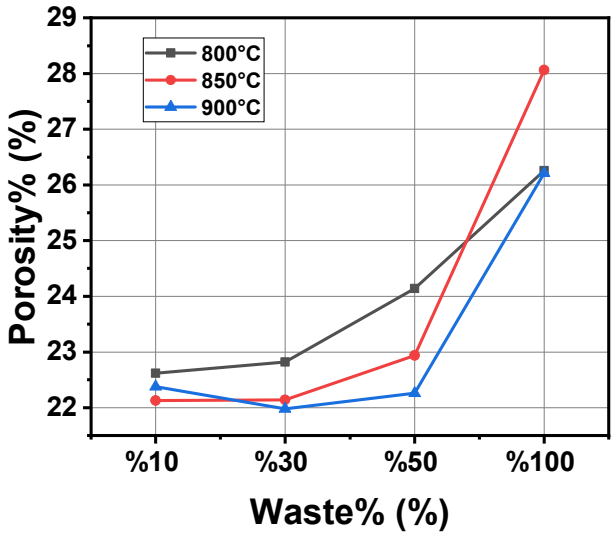

Figure 4. Graph of porosity and waste percentage variation at different temperatures.

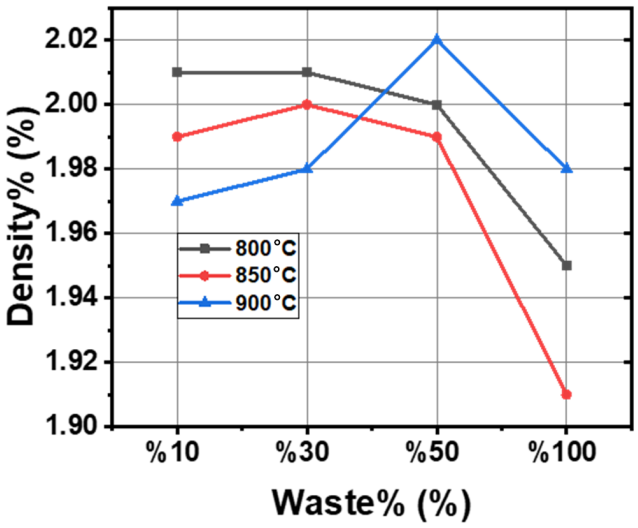

Figure 5. Graph of density and waste percentage variation at different temperatures.

SEM analyses were performed for the samples corresponding to the 10%, 30%, 50%, and 100% mixtures at 800 °C, 850 °C, and 900 °C. As shown in Figure 6, the SEM images corresponding to the 10%, 30%, 50%, and 100% mixtures at 800 °C reveal significant morphological differences linked to composition and process conditions. The SEM images labeled (a), (b), (c), and (d) correspond, respectively, to the samples with increasing percentages (10%, 30%, 50%, and 100%) treated under 800 °C. Notice that with the increase in percentage, definite morphological changes take place.

There is a well-defined microstructure variation in the samples as the percentage increases from 10% to 100%. In Sample (a), the microstructure with 10% is rather sparse, typified by low feature density, less homogeneity in the distribution of particles, and smaller agglomerates. A smooth surface with low porosity and minimal interaction is observed, which can be attributed to the lower percentage of the treated component. However, when the percent increases to 30%, as in Sample b, there is a clear increase in the feature density. With increased material interaction, the distribution becomes more homogeneous, and it can be assumed that this is a transition phase. At 50%, represented by Sample (c), the microstructure transforms very much in the way that there is increased clustering with reduced porosity, and the surface is more interconnected, reflecting enhanced thermal or compositional changes due to the higher percentage. Lastly, at 100%, Sample (d) reveals

a microstructure that is densely packed and well-developed. The surface morphology evidences the highest degree of interaction or reaction, and larger clusters and features indicate full system saturation after treatment at 800 °C.

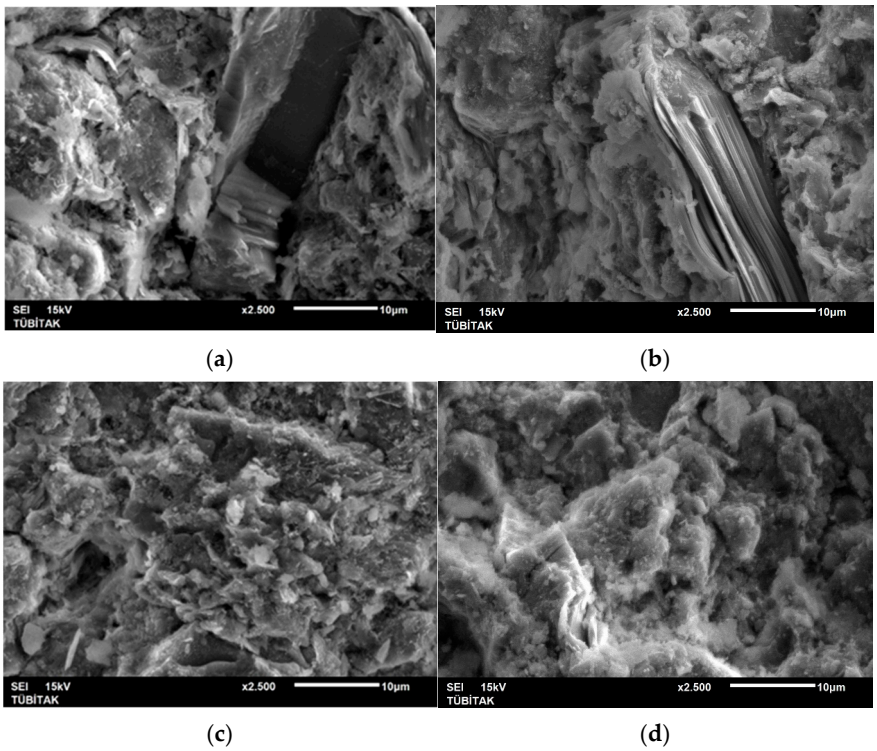

Figure 6. SEM images of the (**a**) 10%,W3S (**b**) 30% W3S, (**c**) 50% W3S, and (**d**) 100% W3S mixtures at 800 °C.

These changes can clearly be followed in the microstructure from 10% in (a) to 100% in (d). Passing through intermediate stages of clustering, one observes that, starting from very sparse and less uniform features in a, the system finally ends up in a very densely packed robust structure for (d). These changes indicate that the percentage directly affects the morphological and, possibly, functional properties of the material; the higher the percentage, the more pronounced the interactions or reactions are under thermal conditions. This phenomenon is related not only to the filling effect but also to enhanced sintering. Additionally, as observed in Table 1, mineralogical analysis indicates the presence of hematite as a newly formed phase in the structure. Therefore, the observed changes in morphology and material properties may also be attributed to the formation of this phase.

The SEM images of the 10%, 30%, 50%, and 100% mixtures of bricks pressed at 25 bar and sintered at 850 °C (Figure 7) reveal progressive densification and structural refinement with increasing sludge content. The microstructure of the samples clearly progresses by increasing the percentage from 10% to 100%. Sample (a), at 10%, is less developed, featuring sparse elements and a minimal tendency toward agglomeration. The particles appear isolated, reflecting a low level of thermal or compositional transformation. At 30%, represented by Sample (b), the density of features increases compared to that in a; the material shows moderate clustering, indicating higher interaction between components with a still relatively dispersed structure. Sample (c), at 50%, shows the most enhanced feature density and connectivity. It gets quite distinctly cluster-characterized and diminishes its void spaces, indicating a tendency for a more coherent behavior by virtue of its higher percentage and thermal treatment. Sample (d) depicts the microstructural attribute of 100%. The complete appearance is of being compacted; high clustering has resulted in nearly

uniform feature density. The material is apparently fully interacted or transformed, thus giving minimal voids and a well-developed and robust surface.

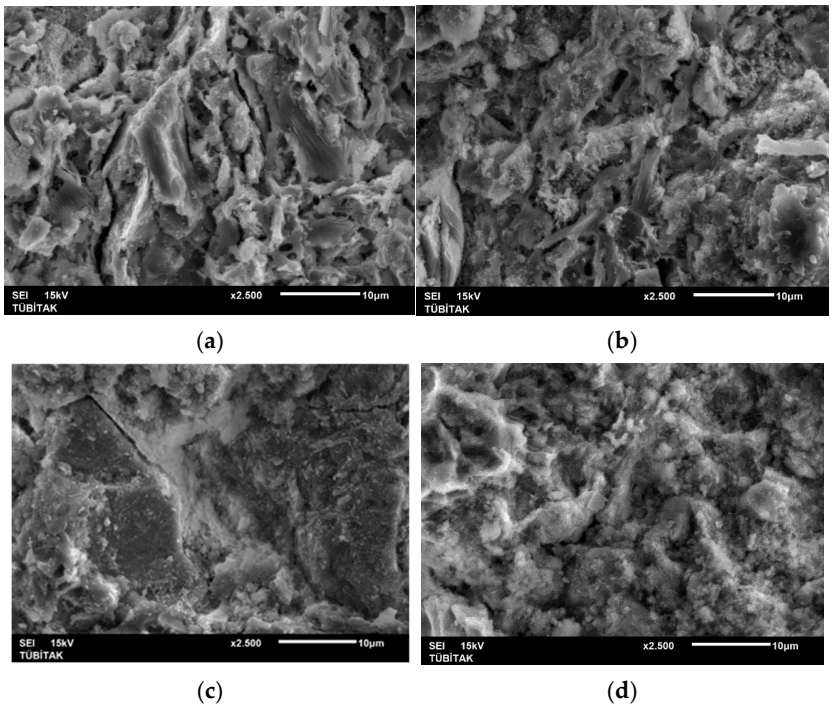

Figure 7. SEM images of the (**a**) 10% W3S, (**b**) 30% W3S, (**c**) 50% W3S, and (**d**) 100% W3S mixtures at 850 °C.

The evolution in Figure 7a–d clearly illustrates the effect of increasing sludge content under identical thermal conditions (850 °C). At 10% (a), the microstructure is sparse and minimally developed, while at 30% (b), the features start to show moderate interaction and clustering. The transformation becomes more pronounced at 50% (c), with the microstructure becoming denser and more cohesive. Finally, at 100% (d), the surface is highly uniform and densely packed, reflecting complete transformation.

The SEM images (Figure 8) of the10 %, 30%, 50%, and 100% mixtures at 900 °C clearly show progression in surface morphology and structural refinement with an increase in the percentage composition. The microstructure of the samples varies significantly with the increase in the percentage from 10% to 100%. Sample (a), at 10%, shows very minimal structural features on the surface, characterized by a sparse particle distribution and very little clustering. The morphology remains reasonably smooth with underdevelopment due to the percentage being lower. At 30%, Sample (b) shows clear-cut clustering, and the feature density is high. This material is in an early stage of major thermal interaction, leading to moderate agglomeration. Sample (c), at 50%, displays more surface structure with better connectivity and enhanced particle clustering. The microstructure is associated with a transitional stage of porosity to homogeneity. Finally, Sample (d), at 100%, re-exposes a very dense surface with a uniform, closely packed microstructure. Clustering is huge with very few voids, and full structural transformation has occurred at this top percentage.

There is a progressive change from 10% to 100%, with regard to percentage, while the sample is maintained at 900 °C. At 10% (a), the surface is sparsely populated and almost undeveloped, and a low interaction has likely prevailed. With an increase to 30% (b), the features are a bit more pronounced and moderately formed in clusters. At 50% (c), the structure acquires a higher density connectivity, which reflects a major transforming phase. Finally, at 100% (d), the material has already acquired a fully developed structure with a dense and uniform surface morphology. These comparisons show the percentage

dependency that influences the thermal behavior and structural evolution of the material. With a higher percentage, the clusterage is more extended, and homogeneity is seen; this also suggests a compositional–microstructural relationship [42].

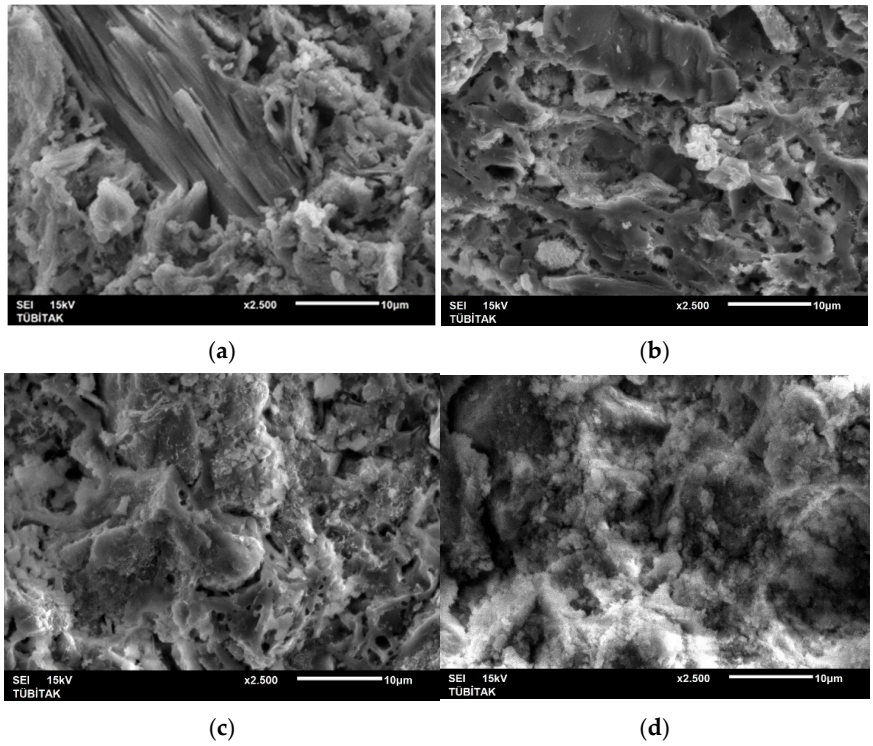

Figure 8. SEM images of the (**a**) 10% W3S, (**b**) 30% W3S, (**c**) 50% W3S, and (**d**) 100% W3S mixtures at 900 °C.

4. Discussion

Analyzing the cumulative graphs as a whole gives strong evidence for how much influence the sludge content and firing temperature have on physical and mechanical brick properties. Generally, compression strength improves with temperature. It has maxima at 900 °C for the bricks with 30% and 50% of the sludge used, signifying that for optimum structural integrity, these two sludge ratios must be used. Total shrinkage and weight loss increased with increasing temperature and sludge content and remained constant above 850 °C. This reflects the thermal effect on dimensional changes. Water absorption and porosity increased linearly with the sludge content, but there was evidence, especially at higher compositions of 50% and 100%, that compactness resulted in a sacrifice of material in moisture retention. Density decreased with the sludge content and showed a slight variation with temperature; this reflects the fact that sludge is lighter compared to clay. These trends highlight that an optimum sludge-to-clay ratio, particularly in the range of 30–50%, together with a firing temperature of 900 °C, is important for mechanical strength, durability, and sustainability in brick production [43,44].

An experimental investigation was performed to study the impact of various contents of sludge and firing temperatures on the mechanical and physical properties of the brick samples. The results of these experiments revealed valuable insights into the interaction between composition, temperature, and microstructural development. Total shrinkage always increased with both higher temperatures and sludge contents. At 800 °C, all the composition series were found to have relatively low values for shrinkage, meaning that minimal contraction occurred in the structure. However, as soon as the temperature reached 850 °C and 900 °C, shrinkage became more pronounced, even for the 30% and 50% sludge

content samples. This progression indicates the thermal-induced densification and phase transformations. Interestingly, for the 100% sludge samples, shrinkage stabilized at 900 °C, which reflects a threshold effect where additional temperature increases did not have any significant influence on the dimensional changes. These observations serve to highlight the need to balance the content of sludge so that there is optimal thermal stability.

Compression strength varied strongly with the sludge content and firing temperature. The highest compression strengths were recorded for the samples with 30% and 50% sludge at 900 °C, thus possessing the best structural properties under these conditions. The 50% sludge sample demonstrated peak performance and, therefore, an ideal balance between porosity and material cohesion. On the other hand, the strength values for the 100% sludge samples were found to fluctuate, decreasing slightly at 850 °C and then increasing at 900 °C. These trends suggest that an excessive sludge content may compromise strength due to increased porosity, highlighting the need for controlled sludge addition to optimize mechanical performance.

Water absorption increased proportionally with the sludge content but remained relatively stable across varying temperatures. The samples with 10% and 30% sludge exhibited the lowest absorption rates, indicating better porosity control and material compactness. In contrast, the 50% and 100% sludge samples achieved higher absorption rates, indicating more open porosity. The porosity values increased in direct proportion with the percentage content of sludge as larger portions of sludge generated more space or voids within the material. There were some indications that at 900 °C, the porosity of the sample with 50% sludge had slightly diminished because of the partial densification effects that usually occur during increased temperature treatment. The constant high porosity of the samples made from 100% sludge at all temperatures reveals the difficulty in achieving compact structures with excessive sludge content. The increase in water absorption with the increase in sludge content is consistent with the findings of Wang et al.'s study [45].

Although the higher sludge content adversely affected the density values, the latter contained lighter sludge compared to clay. On the other hand, minimum effects on density were derived from the firing temperature; even the variations in density were negligible. At all temperatures, the samples with 10% and 30% sludge showed constant density. But the 50% and 100% sludge samples showed small variations. This points out that a trade-off is present between decreased density and mechanical properties because the increased sludge content reduces the compactness of the material [46].

The SEM analyses revealed morphological changes caused by different percentages of sludge and temperatures. At 800 °C, the microstructure was fairly open for lower percentages of sludge but had a denser and more interconnected structure at 50% and 100% sludge. A similar trend was observed at 850 °C and 900 °C, where higher sludge contents led to a higher level of clustering and void spaces. The 50% sludge samples had perfect microstructure formation at 900 °C. There was excellent morphology, which exhibited more intense thermal interaction [47]. On the other hand, the 100% sludge samples presented higher clustering, although they showed increased porosity. Therefore, the complete densification of such samples becomes difficult.

The summary analysis of the entire investigation concludes that there are strong dependencies of brick properties on the sludge concentration and firing temperature. Compression strength increased with temperature, peaking at 900 °C for the 30 and 50 % sludge samples, which had the highest structural performance [48,49]. Shrinkage and weight loss increased with both the temperature and percentage of sludge, but there was stabilization beyond 850 °C, indicating the thermal effects on the overall dimensional changes. The water absorption and porosity trends demonstrated a trade-off in compactness at the expense of moisture retention with higher sludge contents. Meanwhile, the density

results reflected the limit of excessive sludge addition to material compactness and load-carrying capacity.

5. Conclusions

This study has demonstrated the feasibility of incorporating waste silica sand sludge (W3S) as a sustainable additive in brick manufacturing. The findings indicate that the high silica and alumina content of W3S contributes positively to thermal resistance and mechanical stability while simultaneously reducing the presence of fluxing agents such as calcium oxide, sodium oxide, and potassium oxide. Consequently, precise control over the firing conditions is essential to maintaining the structural integrity of the produced bricks.

The experimental approach involved characterizing the physical and chemical properties of both W3S and brick clay, facilitating the design of laboratory-scale experiments. The initial trials with pure brick clay established a reference framework for assessing the influence of W3S incorporation at varying proportions (10%, 30%, 50%, and 100%). The results confirmed that bricks produced with W3S additions exhibited enhanced physical and mechanical properties, validating its potential as an effective raw material substitute.

Among the tested compositions, a 50:50 ratio of W3S and brick clay, fired at 850 °C, emerged as the optimal formulation, offering a balance between mechanical strength, durability, and environmental sustainability. This composition achieved a compressive strength of 126.92 N/mm^2, a relatively low porosity of 22.94%, and a water absorption rate of 11.51%, yielding a dense and durable structure with a stable bulk density of 1.99 g/cm^3. The incorporation of W3S in brick production not only enhances material performance but also provides significant environmental benefits by reducing reliance on virgin clay resources, diverting industrial waste from landfills, and mitigating carbon emissions associated with conventional brick manufacturing processes.

Further observations revealed that bricks containing 10% W3S at 900 °C attained the highest compressive strength, albeit with a lower environmental benefit due to the limited waste utilization. Conversely, bricks composed entirely of W3S exhibited excessive porosity and water absorption, rendering them unsuitable for structural applications. While the 50% W3S mixture at 900 °C performed relatively well, its mechanical strength was slightly lower than that of the same composition fired at 850 °C.

Ultimately, the results underscore the viability of utilizing 50% W3S in brick production at 850 °C as a sustainable waste management strategy. This approach effectively addresses industrial waste disposal challenges while ensuring the production of high-quality construction materials. Future research should focus on evaluating the long-term performance of these materials under real-world environmental conditions to further validate their practical applicability. The broader implications of this study highlight the environmental advantages of repurposing industrial waste in construction, thereby promoting circular economy principles and advancing sustainable building practices.

Funding: This research received no external funding.

Data Availability Statement: The original contributions presented in this study are included in the article. Further inquiries can be directed to the author.

Acknowledgments: I am deeply grateful to Kumsan Foundry Materials Industry and Trade Inc. and Murat Göktuğ Üzümlüoğlu for their raw material support within the scope of this study.

Conflicts of Interest: The author declares no conflicts of interest.

References

1. Wang, S.; Gainey, L.; Mackinnon, I.D.R.; Allen, C.; Gu, Y.; Xi, Y. Thermal behaviors of clay minerals as key components and additives for fired brick properties: A review. *J. Build. Eng.* **2023**, *66*, 105802. [CrossRef]

2. Feiglstorfer, H.; Ottner, F. The impact of clay minerals on the building technology of vernacular earthen architecture in Eastern Austria. *Heritage* **2022**, *5*, 378–401. [CrossRef]
3. Sánchez, D.; Mora, R.; Chaparro, A.; Sánchez-Molina, J. Physicochemical and mineralogical properties of clays used in ceramic industry at North East Colombia. *Dyna* **2019**, *86*, 97–103. [CrossRef]
4. Rosario, M. Advancing sustainable construction: Insights into clay-based additive manufacturing for architecture, engineering, and construction. In *Developments in Clay Science and Construction Techniques*; IntechOpen: Rijeka, Croatia, 2024. [CrossRef]
5. Akintola, G. Mechanical evaluation of soil and artisanal bricks for quality masonry product management, Limpopo, South Africa. *Sci. Rep.* **2024**, *14*, 13921. [CrossRef]
6. Sufian, M.; Ullah, S.; Ostrowski, K.; Ahmad, A.; Zia, A.; Śliwa-Wieczorek, K.; Awan, A. An experimental and empirical study on the use of waste marble powder in construction material. *Materials* **2021**, *14*, 3829. [CrossRef]
7. Pr, F. Synthesis and characterization of clay brick using waste groundnut shell ash. *J. Waste Resour. Recycl.* **2019**, *1*, 101. [CrossRef]
8. Lissy, P.; Peter, C.; Mohan, K.; Greens, S.; George, S. Energy efficient production of clay bricks using industrial waste. *Heliyon* **2018**, *4*, e00891. [CrossRef]
9. Bohara, N.; Bhat, L.; Ghale, D.; Duwal, N.; Bhattarai, J. Investigation of the firing temperature effects on clay brick sample; Part-I: Mineralogical phase characterization. *Bibechana* **2018**, *16*, 122–130. [CrossRef]
10. Johari, I.; Saıd, S.; Hisham, B.; Bakar, A.; Ahmad, Z. Effect of the change of firing temperature on microstructure and physical properties of clay bricks from Beruas (Malaysia). *Sci. Sinter.* **2010**, *42*, 245–254. [CrossRef]
11. Khanal, D.; Paudel, M.R. Quality assessment of bricks produced in Chitwan District, Central Nepal. *J. Nepal Geol. Soc.* **2023**, *65*, 141–150. [CrossRef]
12. Teklehaimanot, M.; Hailay, H.; Tesfaye, T. Manufacturing of ecofriendly bricks using microdust cotton waste. *J. Eng.* **2021**, *2021*, 8815965. [CrossRef]
13. Raut, S.; Ralegaonkar, R.; Mandavgane, S. Development of sustainable construction material using industrial and agricultural solid waste: A review of waste-create bricks. *Constr. Build. Mater.* **2011**, *25*, 4037–4042. [CrossRef]
14. Tessema, I. Production and characterization of bricks from bottom ash and textile sludge using plastic waste as binding agent. *J. Eng.* **2023**, *2023*, 7607677. [CrossRef]
15. Chin, W.; Lee, Y.; Amran, M.; Fediuk, R.; Vatin, N.; Kueh, A.; Lee, Y. A sustainable reuse of agro-industrial wastes into green cement bricks. *Materials* **2022**, *15*, 1713. [CrossRef]
16. Ongpeng, J.; Inciong, E.; Sendo, V.; Soliman, C.; Siggaoat, A. Using waste in producing bio-composite mycelium bricks. *Appl. Sci.* **2020**, *10*, 5303. [CrossRef]
17. Singh, A.; Srivastava, A.; Singh, A.; Singh, H.; Kumar, A.; Singh, G. Utilization of plastic waste for developing composite bricks and enhancing mechanical properties: A review on challenges and opportunities. *Adv. Polym. Technol.* **2023**, *2023*, 6867755. [CrossRef]
18. Weng, C.; Lin, D.; Chiang, P. Utilization of sludge as brick materials. *Adv. Environ. Res.* **2003**, *7*, 679–685. [CrossRef]
19. Chen, C.; Wu, H. Lightweight bricks manufactured from ground soil, textile sludge, and coal ash. *Environ. Technol.* **2017**, *39*, 1359–1367. [CrossRef]
20. Uslu, E.; Avşar, E.; Toröz, İ. Otomotiv Endüstrisi Kimyasal Arıtma Çamurlarının Tuğla Üretiminde Kullanılabilirliğinin Ürün Kalitesi Yönünden Araştırılması. In Proceedings of the TÜRKAY 2009: Türkiye'de Katı Atık Yönetimi Sempozyumu, İstanbul, Türkiye, 15–17 June 2009.
21. Adiyanto, O.; Mohamad, E.; Razak, J. Systematic review of plastic waste as eco-friendly aggregate for sustainable construction. *Int. J. Sustain. Constr. Eng. Technol.* **2022**, *13*, 243–257. [CrossRef]
22. Shubbar, A.; Sadique, M.; Kot, P.; Atherton, W. Future of clay-based construction materials—A review. *Constr. Build. Mater.* **2019**, *210*, 172–187. [CrossRef]
23. Odeyemi, S. Determining the Properties of Unfired Stabilized Kaolinitic Clay Brick for Sustainable Construction. *Key Eng. Mater.* **2024**, *981*, 237–246. [CrossRef]
24. Ariq, O. Development of Geothermal Sludge Derived-Silica Catalyst for Sago Starch Hydrolysis. *Key Eng. Mater.* **2024**, *6*, 37–41. [CrossRef]
25. Suhadi, E. Preparation of Sulfonated SiO_2 Catalyst from Geothermal Sludge Waste for Sago Flour Hydrolysis. *Adv. Sci. Technol.* **2024**, *138*, 71–75. [CrossRef]
26. Adiatama, A.; Susanti, R.; Astuti, W.; Petrus, H.; Wanta, K. Synthesis and Characteristic of Nanosilica from Geothermal Sludge: Effect of Surfactant. *Metalurgi* **2022**, *37*, 73. [CrossRef]
27. Şenol, A.; Guner, A. Use of Silica Fume, Bentonite, and Waste Tire Rubber as Impermeable Layer Construction Materials. *Adv. Civ. Eng.* **2023**, *2023*, 7301343. [CrossRef]
28. Kuok, C.H.; Dianbudiyanto, W.; Liu, S.H. A Simple Method to Valorize Silica Sludges into Sustainable Coatings for Indoor Humidity Buffering. *Sustain. Environ. Res.* **2022**, *32*, 8. [CrossRef]

29. Judith, J.V.; Vasudevan, N. Synthesis of Nanomaterial from Industrial Waste and Its Application in Environmental Pollutant Remediation. *Environ. Eng. Res.* **2022**, *27*, 200672. [CrossRef]
30. Salman, A.D.; Juzsakova, T.; Le, P.C.; Jalhoom, M.G.; Abdullah, T.A.; Domokos, E.; Le, H.-S.; Chang, S.W.; Kim, S.C.; Nguyen, D.D. Preparation, Characterization, and Application of Nano-Silica from Agricultural Wastes in Cement Mortar. Biomass Convers. *Biomass Convers. Biorefin.* **2023**, *13*, 9411–9421. [CrossRef]
31. Anjum, F.; Ghaffar, A.; Jamil, Y.; Majeed, M.I. Effect of sintering temperature on mechanical and thermophysical properties of biowaste-added fired clay bricks. *J. Mater. Cycles Waste Manag.* **2019**, *21*, 503–524. [CrossRef]
32. Ahmad, S.; Iqbal, Y.; Muhammad, R. Effects of coal and wheat husk additives on the physical, thermal and mechanical properties of clay bricks. *Bol. Soc. Esp. Cerám. Vidr.* **2017**, *57*, 131–138. [CrossRef]
33. Mgbemere, H.E.; Obidiegwu, E.O.; Ubong, A.U. The Effects of Sintering Temperature and Agro Wastes on the Properties of Insulation Bricks. *Niger. J. Technol. Dev.* **2020**, *17*, 113–119. [CrossRef]
34. Rossi, F.; Telesca, A.; Marroccoli, M.; Valenti, G.L.; Sersale, R. Effect of sludge content on water absorption and porosity in artificial stone slabs. *Constr. Build. Mater.* **2015**, *78*, 197–204. [CrossRef]
35. Correia, S.L.; Segadães, A.M.; Labrincha, J.A. Incorporation of sewage sludge in ceramic materials: Influence on porosity and durability. *Materials* **2014**, *17*, 5625. [CrossRef]
36. Amin, M.; Abdel-Rahman, H.; Salama, R. Utilization of water treatment sludge as a partial replacement in sustainable construction materials. *Sustainability* **2023**, *15*, 9389. [CrossRef]
37. Baspinar, M.S.; Demir, I.; Orhan, M. Utilization potential of silica fume in fired clay bricks. *Waste Manag. Res.* **2007**, *25*, 546–552. [CrossRef]
38. Amin, M.; Abdel-Rahman, H.; Salama, R. Potential use of water treatment sludge as partial replacement for clay in eco-friendly bricks. *Sustainability* **2023**, *15*, 9389.
39. Kadir, A.A.; Rahim, S.A. An overview of sludge utilization into fired clay brick. *Int. J. Environ. Sci. Dev.* **2012**, *3*, 497–500.
40. Romero, R.; Morales, M.P.; Pérez, J.F. *Effects of Coal and Wheat Husk Additives on the Properties of Fired Clay Bricks*; Boletín de la Sociedad Española de Cerámica y Vidrio; Elsevier: Amsterdam, The Netherlands, 2017.
41. Fernández, R.; Martín-Márquez, J.; Rincón, J.M.; Romero, M. *Effects of Temperature on the Sintering Behavior of Clay-Based Ceramics with Additions of İndustrial Wastes*; PMC—National Library of Medicine: Bethesda, MD, USA, 2011.
42. Wang, S.; Gainey, L.; Baxter, D.; Wang, X.; Mackinnon, I.D.R.; Xi, Y. Thermal behaviours of clay mixtures during brick firing: A combined study of in-situ XRD, TGA and thermal dilatometry. *Constr. Build. Mater.* **2021**, *299*, 124319. [CrossRef]
43. Nor, M.; Hamed, A.; Ali, F.; Khim, O. Properties and Performance of Water Treatment Sludge (WTS)-Clay Bricks. *J. Teknol.* **2015**, *77*. [CrossRef]
44. Ge, H. Review of Solid Waste Resource Utilization for Brick-Making. *E3S Web Conf.* **2024**, *520*, 02006. [CrossRef]
45. Wang, S.; Gainey, L.; Mackinnon, I.D.R.; Xi, Y. High- and low-defect kaolinite for brick making: Comparisons of technological properties, phase evolution and microstructure. *Constr. Build. Mater.* **2023**, *366*, 130250. [CrossRef]
46. Ewemoje, O.; Bademosi, T. Development of a Sludge Dewatering Filter and Utilization of Dried Sludge in Brick Making. *Fuoye J. Eng. Technol.* **2019**, *4*, 76–81. [CrossRef]
47. Huang, B.; Zhang, X.; Zhu, J.Z. Influence of Sludge Content on Compressive Strength of Sintering Sludge-Shale Bricks. *Appl. Mech. Mater.* **2012**, *238*, 101–104. [CrossRef]
48. Amin, F.; Abbas, S.; Abbass, W.; Salmi, A.; Ahmed, A.; Saeed, D.; Sufian, M.; Sayed, M.M. Potential Use of Wastewater Treatment Plant Sludge in Fabrication of Burnt Clay Bricks. *Sustainability* **2022**, *14*, 6711. [CrossRef]
49. Zhang, X.; Jiao, Y.; Yu, L.; Liu, H.; Wang, X. Effect of Sewage Sludge Addition on Microstructure and Mechanical Properties of Kaolin-Sewage Sludge Ceramic Bricks. *Coatings* **2022**, *12*, 944. [CrossRef]